European Journal of Medicinal Chemistry 44 (2009) 4793–4800

Contents lists available at ScienceDirect

European Journal of Medicinal Chemistry

journal homepage: http://www.elsevier.com/locate/ejmech

Original article

Discovery of potential ZAP-70 kinase inhibitors: Pharmacophore design, database screening and docking studies

Ramadevi Sanam [a,b,*], S. Vadivelan [a], Sunita Tajne [a], Lakshmi Narasu [b], G. Rambabu [a], Sarma A.R.P. Jagarlapudi [a]

[a] GVK Biosciences Pvt. Ltd., Informatics Division, S-1, Phase-1, T.I.E. Balanagar, Hyderabad, Andhra Pradesh 500037, India
[b] School of Biotechnology, Jawaharlal Nehru Technological University, Kukatpally, Hyderabad, Andhra Pradesh 500072, India

ARTICLE INFO

Article history:
Received 5 December 2008
Received in revised form
1 June 2009
Accepted 16 July 2009
Available online 21 July 2009

Keywords:
ZAP-70
Pharmacophore
HypoGen model
Virtual screening
Docking

ABSTRACT

The best ZAP-70 inhibitor model consists of four-pharmacophore features, (1) one hydrogen bond acceptor, (2) one hydrogen bond donor (3) one hydrophobic aliphatic and (4) one hydrophobic aromatic features. This model was validated against 110 known ZAP-70 inhibitors with a correlation of 0.902 as well as enrichment factor of 1.61 against a maximum value of 2. This model picked 4094 hits from a database of 238,819 molecules while 358 molecules were indicated as highly active. Subsequently, docking studies were performed on the hits and novel series of potent leads were suggested based on the interactions energy between ZAP-70 and the putative inhibitors which validated not only the virtual screening potential of the model but also identified the possible new Chemotypes.

1. Introduction

Protein tyrosine kinase activation, and the subsequent phosphorylation of multiple cellular substrates, is the earliest of the known biochemical events associated with T-cell activation. Inhibitors of lymphocyte activation are of potential use for treatment of a variety of human diseases such as transplant rejection, allergic responses, autoimmune disorders, and inflammation. ZAP-70 kinase, a 70 kDa member of the Syk family kinase associated with the ζ-subunit of the T-cell receptor, is primarily expressed in T and NK cells and plays an important role in the initiation of normal TCR signaling, crucial for T-cell activation and development. The relative importance of this kinase for lymphocyte activation has been evaluated by disrupting functional ZAP-70 which resulted in a marked reduction in protein tyrosine phosphorylation, cytosolic Ca^{2+} level change, and loss of of IL-2 production, demonstrating that ZAP-70 is absolutely required for IL-2 production by T-cells [1–3]. In addition, human severe combined immunodeficiency patients have been identified that who do not express ZAP-70 protein [4,5]. All these reports indicate that ZAP-70 is a potentially useful therapeutic target for immune suppression. Inhibitors of ZAP-70 tyrosine kinase activity with high affinity and high selectivity can block signaling downstream of the kinase leading to inhibition of T-cell lymphocyte activation. Peptides that block the association of ZAP-70 with the ζ-subunit and compounds that antagonize ZAP-70 tyrosine kinase activity are known to block T-cell activation in vitro [6–11]. Piceatannol blocks Syk and ZAP-70 tyrosine kinases involved in immune cell activation and prolong kidney allograft survival in the stringent ACI-to-Lewis rat model [7]. The three-dimensional structure of the catalytic tyrosine kinase domain of ZAP-70 has been crystallized recently in complex with Staurosporine at 2.3 Å resolution. Staurosporine is a non-selective, ATP inhibitor of many kinases having IC_{50} value of 55.8 nM against rhZAP-70 tyrosine kinase [8]. There is currently no highly specific, small-molecule inhibitor for ZAP-70. In situations where overactive T-cells are a substantial component of disease, such as in autoimmune diseases or transplantation, targeting ZAP-70 could provide a means to target the T-cells while avoiding adverse effects on other cells. Thus, a potent and selective ZAP-70 tyrosine kinase inhibitor should modulate T-cell function in a more targeted fashion than the less specific immunosuppressive agents currently available, such as cyclosporine A and FK-506. In virtual screening, computational models are used to predict the biological activity of compounds. The computational models can be generated and validated utilizing either the 3D structure of the target or a set of active analogues

* Corresponding author. GVK Biosciences Pvt. Ltd., Informatics Division, S-1, Phase-1, T.I.E. Balanagar, Hyderabad, Andhra Pradesh 500037, India. Tel.: +91 40 23721001; fax: +91 40 23721010.
E-mail address: ramadevi.sanam@gvkbio.com (R. Sanam).

0223-5234/$ – see front matter © 2009 Elsevier Masson SAS. All rights reserved.
doi:10.1016/j.ejmech.2009.07.018

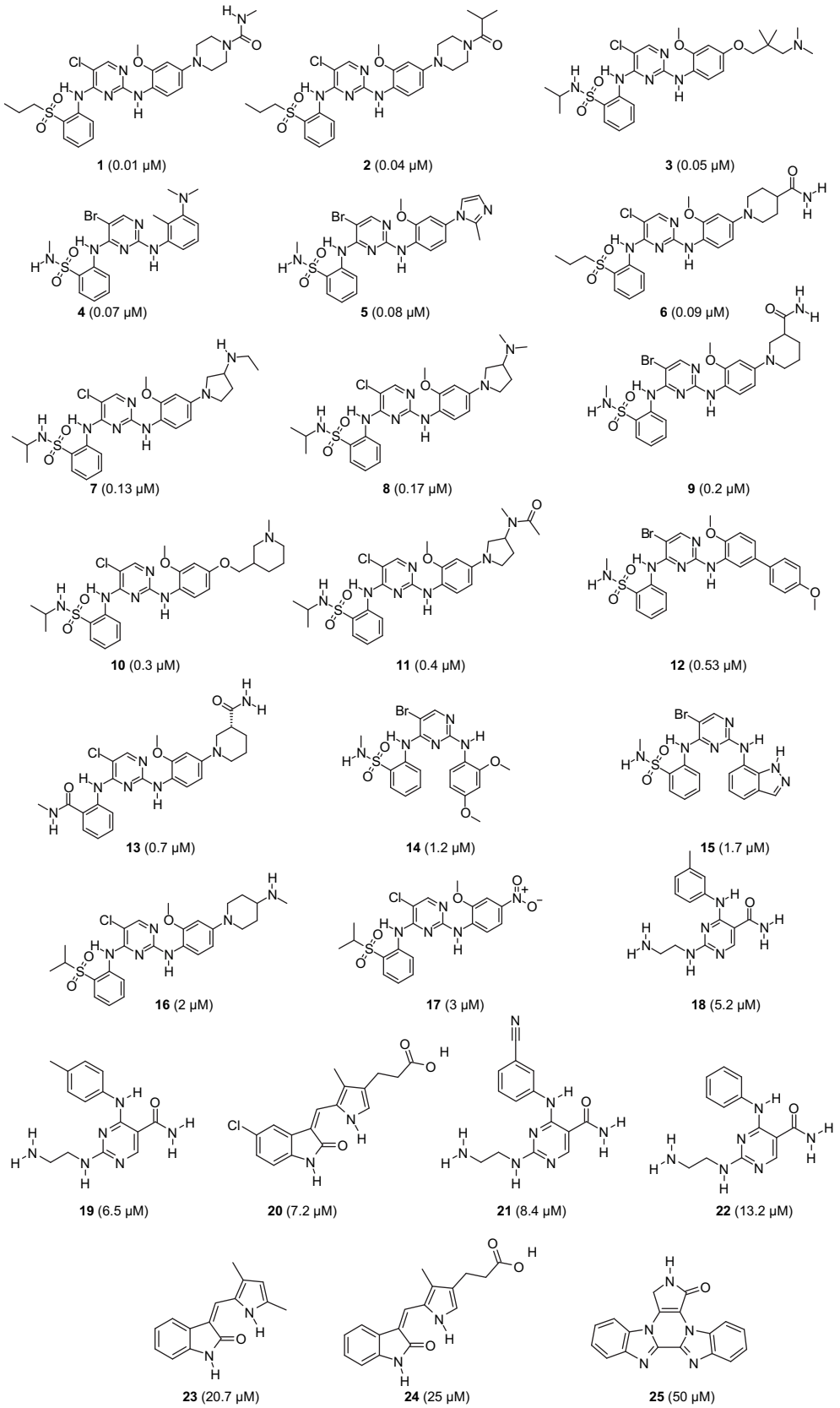

Fig. 1. Training set molecules for ZAP-70 inhibitors. IC_{50} values of each molecule are given in parentheses.

specific to the target. In this study, we had discussed about the pharmacophore and concurrent docking studies and finally the validated model is used to screen the library to discover a set of novel ZAP-70 inhibitors.

2. Computational details

2.1. Pharmacophore studies using Catalyst

Pharmacophore modeling correlates activities with the spatial arrangement of various chemical features in a set of active analogues. A set of 135 human ZAP-70 inhibitors [9–13] with an activity range (IC_{50}) spanning over 5 orders of magnitude i.e. 0.1–50 μM was selected. This initial group was then divided into the training and test sets. The training set of 25 molecules was designed to be structurally diverse with a wide activity range. All the training set compounds from the literature have similar ZAP-70 inhibitory assay. Assay conditions were also taken into consideration. Molecules with K_i, ED_{50}, EC_{50} and other activity type values were ignored and not considered for modeling studies. The training set molecules play a critical role in the pharmacophore generation process and the quality of the resultant pharmacophore models relies solely on the training set molecules. The test set of remaining 110 molecules is designed to evaluate predictive ability of the resultant pharmacophore. Highly active, moderately active, and inactive compounds were added to the training set to obtain critical information on pharmacophoric requirements for ZAP-70 inhibition. The molecules selected as the training set are given in Fig. 1 and a few molecules from the test set are given in Fig. 2. This training set was then used to generate quantitative pharmacophore models.

Qualitative pharmacophore models were generated using a set of highly active molecules. Common feature hypotheses (qualitative models) were produced by comparing a set of conformational models with a number of 3D configurations of chemical features shared among the training set molecules. This analysis results in a qualitative model wherein important chemical features can be easily identified. For chemically meaningful patterns, it is important to identify such chemical features before proceeding to the quantitative model generation process. To confirm essential features prevailing among the ZAP-70 inhibitors, 10 common feature hypotheses were generated using the most active molecules **1**–**6** (Fig. 1). The common features for all 10 hypotheses are hydrogen bond donor, hydrogen bond acceptor and hydrophobic features. However, these models cannot be directly used to predict biological activity of the compounds retrieved from a database. We have generated quantitative pharmacophore models to predict the biological activities of novel compounds. For the quantitative model generation, 25 training set compounds with structural diversity were taken and classified as highly active (<0.5 μM), moderately active (0.5–5 μM) and inactive (>5 μM). While generating the quantitative model, a minimum of 0 to a maximum of 5 features involving HBA, HBD, and HA features were selected and used to build a series of hypotheses using a default uncertainty value of 3. The quality of HypoGen models is best described in Catalyst user guide [14] in terms of fixed cost, null cost and total cost and other statistical parameters. According to which, a large difference between the fixed cost and null cost, and a value of 40–60 bits for the unit of cost would imply a 75–90% probability for experimental and predicted activity correlation. In general, pharmacophore models should be statistically significant, predict the activity of molecules accurately, and retrieve active compounds from a database. The derived pharmacophore models were validated using a set of parameters including cost analysis, test set prediction, enrichment factor, and goodness of hit. HipHop and HypoGen modules within Catalyst were then used to generate qualitative pharmacophore and quantitative pharmacophore models, respectively [15–17].

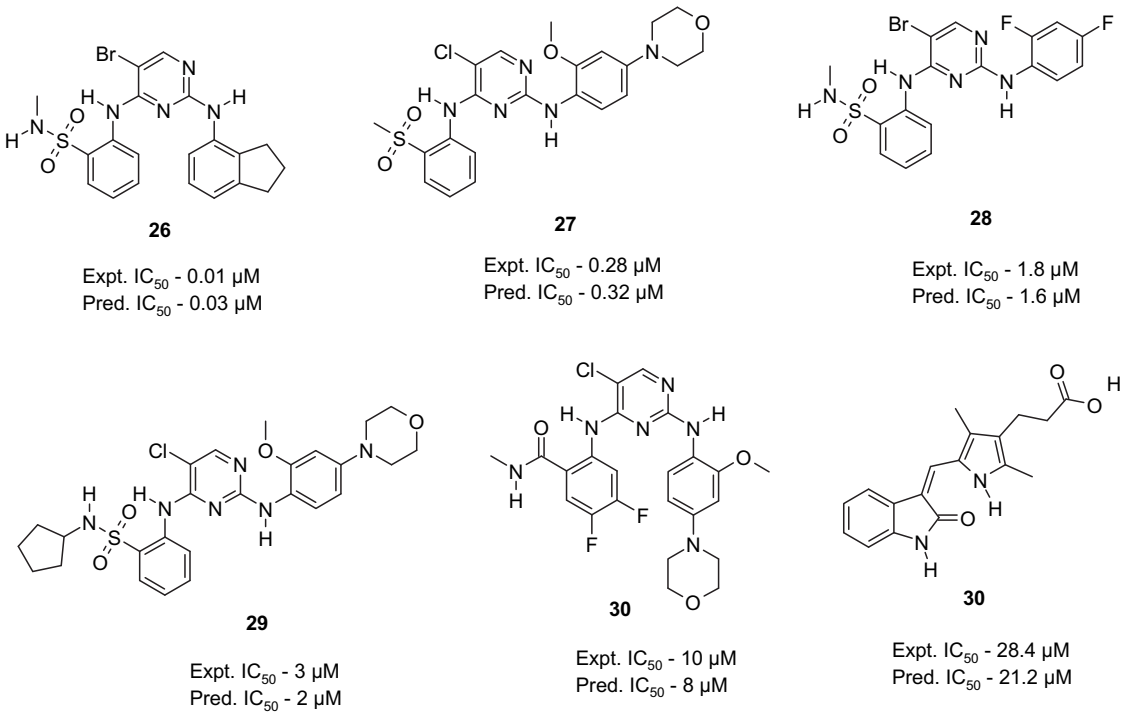

Fig. 2. Some test set molecules for ZAP-70 inhibitors along with its experimental and pharmacophore predicted IC_{50} values.

2.2. Docking studies using GOLD

Crystal structure of ZAP-70 (PDB code: 1U59) was used for the study. The protein 3D structure was downloaded from the protein databank (PDB) [18], the solvent molecules in the protein were removed and hydrogen atoms were added to the protein using Cerius^2 module [19]. Structure-based docking studies were carried out using GOLD [20] version 3.0 on 135 minimized ZAP-70 inhibitors and on hits/leads from virtual screening to the ATP-binding site of ZAP-70 complex. The active site was defined as the region within 12 Å from the geometric centroid of ligand ($X = 11.6$, $Y = 5.09$ and $Z = 53.58$) complexed with the protein ZAP-70. Default settings for small molecule–protein docking were used throughout simulations. For each of the 10 independent genetic algorithm runs, with a selection pressure of 1.1, 100,000 operations were performed on a set of 5 islands with a population size of 100 individuals. Standard operator weights were used for crossover, mutation, and migration of 95, 95, and 10, respectively. Cut-off values of 2.5 Å for H-bonds and 4.0 Å for van der Waals were employed. Top 50 poses were collected for each molecule. The best docked score value for each molecule associated with a favorable binding conformation compared to the co-crystallized inhibitor was considered to correlate with biological activity. Highly active hits retrieved from the virtual screening libraries were further refined by performing docking studies with the molecules.

3. Results and discussion

3.1. Pharmacophore generation and validation studies

The best common feature pharmacophore model [21] indicated the importance of H-bond acceptor (HBA), H-bond donor (HBD), hydrophobic aliphatic (HA) and hydrophobic aromatic (HRA) features, as shown in Fig. 3A, which were further confirmed in the quantitative models. Several quantitative models were generated utilizing the training set (**1**–**25**) along with ZAP-70 inhibitory activities (Fig. 1 and Table 1). The top ten hypotheses were composed of HBA, HBD, and HRA features. The values of ten hypotheses such as cost, correlation (r), and root-mean-square deviations (rmsd) are statistically significant (Table 2). It is evident that as error, weight and configuration components are very low and not deterministic to the model; the total pharmacophore cost is also low and close to the fixed cost. Also, as total cost is less than the null cost, this model accounts for all the pharmacophore features and has good predictive ability. In addition to an estimation of activity of the training set molecules, the pharmacophore model should also accurately predict activity of the test set molecules. Two statistical methods were employed to rank the ten resultant hypotheses. In the first method, all ten hypotheses were evaluated using a test set of 110 known ZAP-70 inhibitors, which are not included in the training set. Predicted activities of the test set were calculated using all ten hypotheses and correlated with experimental activities. Of the ten hypotheses, Hypo1 showed a better

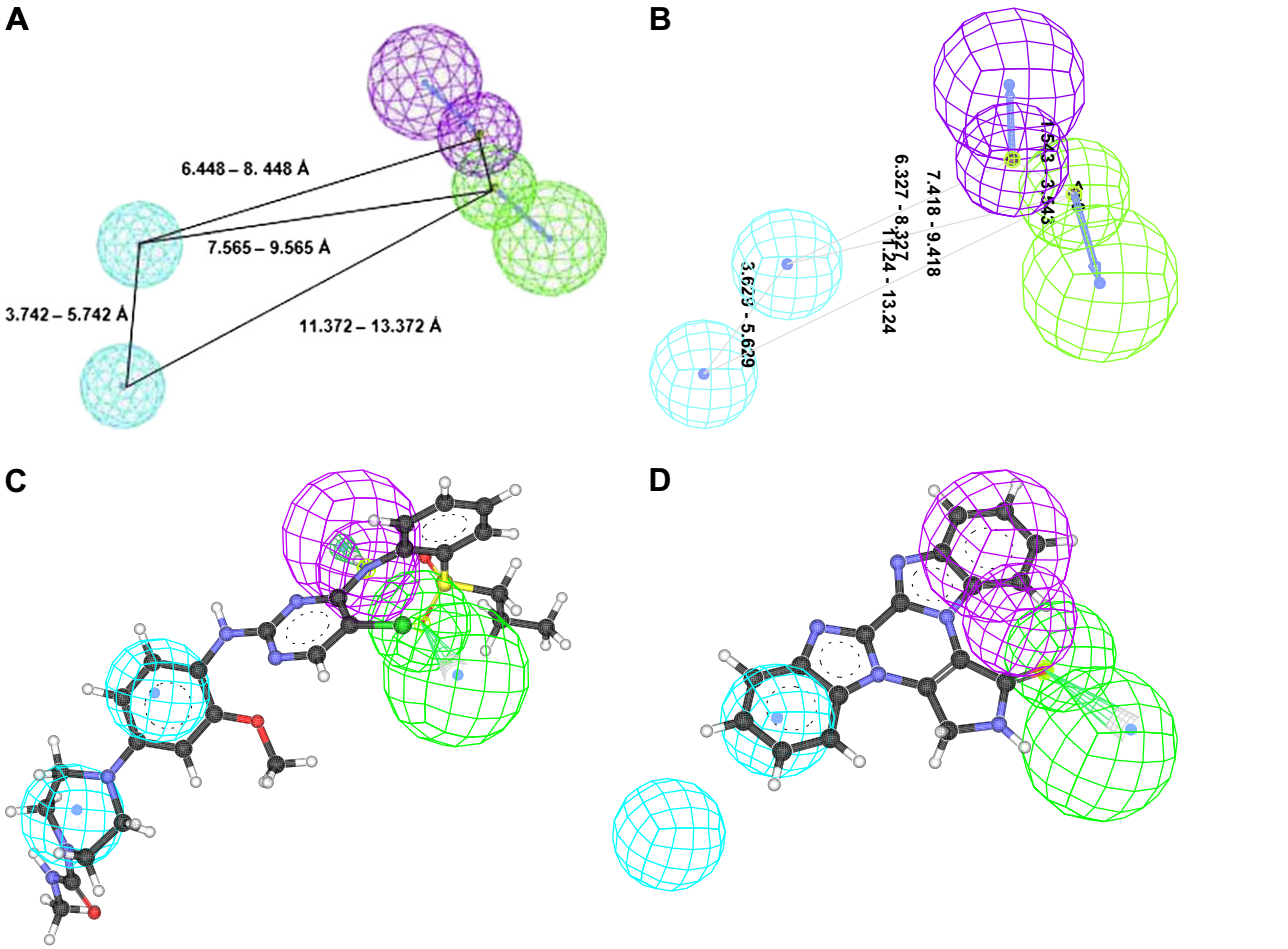

Fig. 3. Pharmacophore models for ZAP-70 inhibitors. A. HipHop features with its distance constraints. B. HypoGen features with its distance constraints. C. Pharmacophore mapped to the most active molecule (1, 0.01 μM). D. Pharmacophore mapped to the low-active molecule (25, 50 μM). Features are color coded with green: one hydrogen bond acceptor, magenta: hydrogen bond donor and light blue: hydrophobic aliphatic and aromatic.

Table 1
Experimental and predicted IC_{50} data of 25 training set molecules against HypoGen model.

Molecule	Exp. IC_{50}, μM	Predicted IC_{50}, μM	Error[a]	Fit value[b]	Experimental scale[c]	Predicted scale[c]
1	0.01	0.0083	−1.2	6.55	+++	+++
2	0.04	0.059	1.5	5.7	+++	+++
3	0.05	0.054	1.1	5.74	+++	+++
4	0.07	0.32	4.6	4.97	+++	+++
5	0.08	0.057	−1.4	5.72	+++	+++
6	0.09	0.084	−1.1	5.55	+++	+++
7	0.13	0.43	3.3	4.84	+++	+++
8	0.17	0.15	−1.2	5.31	+++	+++
9	0.2	0.16	−1.2	5.26	+++	+++
10	0.3	0.3	−1	5	+++	+++
11	0.4	0.35	−1.1	4.93	+++	+++
12	0.53	0.35	−1.5	4.93	++	+++
13	0.7	0.51	−1.3	4.82	++	++
14	1.2	0.67	−1.8	4.9	++	++
15	1.7	0.57	−3	4.72	++	++
16	2	1.8	−1.1	4.22	++	++
17	3	3.7	1.2	3.9	++	++
18	5.2	8.7	1.7	3.39	+	+
19	6.5	10.5	1.6	3.38	+	+
20	7.6	14.6	1.9	3.38	+	+
21	8.4	12.7	1.5	3.39	+	+
22	13	13	−1	3.36	+	+
23	21	31	1.4	3.36	+	+
24	25	19	−1.3	3.38	+	+
25	50	40	−1.3	3	+	+

[a] + indicates that the predicted IC_{50} is higher than the experimental IC_{50}; − indicates that the predicted IC_{50} is lower than the experimental IC_{50}; a value of 1 indicates that the predicted IC_{50} is equal to the experimental IC_{50}.

[b] Fit value indicates how well the features in the pharmacophore overlap the chemical features in the molecule. Fit = weight × [max(0.1 − SSE)] where SSE = $(D/T)2$, D = displacement of the feature from the center of the location constraint and T = the radius of the location constraint sphere for the feature (tolerance).

[c] Activity scale – $IC_{50} < 0.5$ μM = +++ (highly active) – IC_{50} 0.5–5 μM = ++ (moderately active) – $IC_{50} > 5$ μM = + (low active).

correlation coefficient (0.972) compared to the other nine hypotheses. A second statistical test includes calculation of false positives, false negatives, enrichment, and goodness of hit to determine robustness of hypotheses. Under all validation conditions, Hypo1 performed superior as compared to the other nine hypotheses (Fig. 3B). Hypo1 demonstrated excellent prediction of ZAP-70 inhibitory activities of the training set compounds (Table 1). Analyzing the results, it was observed that out of 11 highly active molecules, all were predicted correctly as highly active. Among the 6 moderately active molecules, except one, which was predicted as highly active and the rest were correctly predicted. Out of 8 low-active molecules all of them were predicted as low active. Activities of the compounds were not only correctly predicted, but the fit values also confer a good measure of how well the pharmacophoric features of Hypo1 were mapped onto the chemical features of the compounds. Fig. 3A shows the HypoGen pharmacophore features with their geometric parameters and all features of Hypo1 (HBA, HBD, HA and HRA) were mapped onto the highly active compounds of the training set (Fig. 3C, molecule **1** in Fig. 3B). Many of the inactive compounds in the training set did not map onto one or more features of Hypo 5 (see for example molecule **25** in Fig. 3D).

The correlation values along with the predictions above make the pharmacophore suitable to predict molecular properties well. The plot showing the correlation between the actual and predicted activities for the test set and the training set molecules is given in Fig. 4. This indicates that the pharmacophore model generated is capable of predicting the activity of the unknown molecules with reasonable accuracy.

The purpose of the pharmacophore model generation is not just to predict the activity of the training set compounds accurately but also to verify whether the pharmacophore models are capable of predicting the activities of external compounds of the test set series and classifying them correctly as active or inactive. Hypo1 was used to search the test set of known ZAP-70 inhibitors. Database mining was performed using the BEST flexible searching technique. The results were analyzed using a set of parameters [22] such as hit list (Ht), number of active percent of yields (%Y), percent ratio of actives in the hit list (%A), enrichment factor (E), false negatives, false positives, and goodness of hit score (GH) (Table 3). Hypo1 succeeded in the retrieval of 90% of the active compounds from the test set. In addition, the pharmacophore also retrieved 6 inactive compounds (false positives). It predicted 3 active compounds as inactive (false negatives). An enrichment factor of 1.61 and a GH score of 0.80 indicate the quality of the model. Overall, a strong correlation was observed between the Hypo1 predicted activity and the experimental ZAP-70 inhibitory activity (pIC_{50}) of the training and test set compounds (Fig. 4). However, the Hypo1 model has a greater tendency to show false positives. This could be attributed to high structural similarity in active and inactive ZAP inhibitors, resulting in an inability to discriminate this pattern by the pharmacophore model. We further extended this study to structure-based design and to limit the number of false positive and false negative hits and to further understand the binding of inhibitors to the active site of ZAP-70 complex.

Table 2
10 Pharmacophore models generated by the HypoGen for ZAP-70 inhibitors.

Hypo no.	Total cost	Cost difference[a]	Error cost	RMS deviation	Training set (r)	Features[b]
1	108.18	56.16	87.98	0.558	0.972	ADHAHRA
2	108.28	56.06	88.41	0.588	0.958	ADHAHRA
3	109.17	55.17	89.42	0.653	0.948	ADHAHRA
4	109.17	55.17	89.48	0.657	0.947	ADHAHRA
5	109.64	54.7	89.95	0.685	0.943	ADHAHRA
6	109.83	54.51	90.13	0.695	0.941	ADHAHRA
7	110.26	54.08	90.47	0.715	0.938	ADHAHRA
8	110.31	54.03	90.48	0.714	0.938	ADHAHRA
9	110.53	53.81	90.84	0.735	0.934	ADHAHRA
10	110.68	53.66	90.98	0.742	0.933	ADHAHRA

[a] (Null cost − total cost), null cost = 164.34, fixed cost = 103.75, for the Hypo1 weight = 1.84, configuration = 14.84. All cost units are in bits.

[b] A – hydrogen bond acceptor, D – hydrogen bond donor, HA – hydrophobic aliphatic and HRA – hydrophobic aromatic.

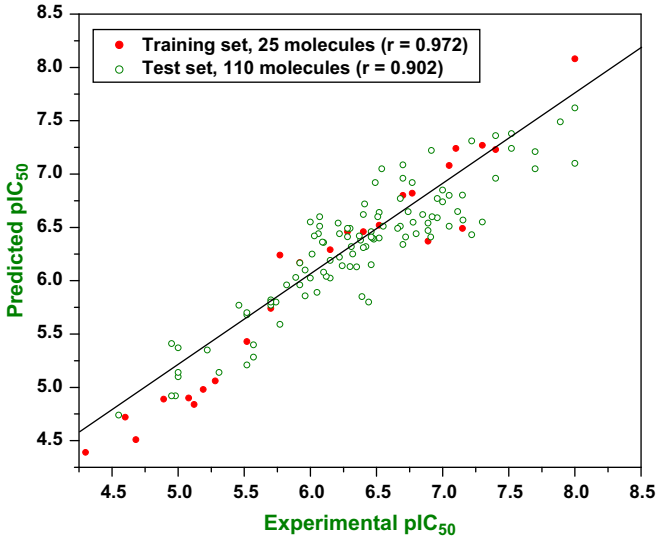

Fig. 4. Graph showing the correlation (r) between experimental and predicted activities for the 110 test set molecules against Hypo1 model along with 25 training set molecules for ZAP-70 inhibitors.

Table 3
Statistical parameters from screening of test set molecules.

S. no	Parameter	ZAP-70[a]
1	Total molecules in database (*D*)	110
2	Total number of actives in database (*A*)	62
3	Total hits (Ht)	65
4	Active hits (Ha)	59
5	% Yield of actives [(Ha/Ht) × 100]	90.7
6	% Ratio of actives [(Ha/*A*) × 100]	95.1
7	Enrichment factor (*E*) [(Ha × *D*)/(Ht × *A*)]	1.61
8	False negatives [*A* − Ha]	3
9	False positives [Ht − Ha]	6
10	Goodness of hit score[a]	0.80

[a] [(Ha/4Ht*A*) (3*A*+Ht)) × (1 − ((Ht − Ha)/(*D* − *A*))]; GH score of 0.7–0.8 indicates a very good model.

3.2. Database screening

The Hypo1 model was used as a query to screen NCI database consisting of 238,819 molecules, and retrieved 4094 hits (1.7% of database) comprising 358 high, 1352 medium and 2384 low-active molecules. The high active molecules were those <0.5 μM, moderately active (0.5–5 μM) and low active (>5 μM). Only 42 hits are found to be having activities below the 0.1 μM cut-offs. In fact, one can consider all the 358 hits that are predicted as highly active could become a good source for further evaluation, while some others in medium actives cannot be completely neglected. Some of the hits with good predicted activities were further subjected to docking studies to reduce the number of false positives and false negatives. Based on the earlier observations and the model developed in this study, it is observed that this virtual screening effort produced relatively more hits on which further experimental studies could be carried out. A few of the lead molecules with high predicted activity and fitness score are given in Fig. 5.

3.3. Docking studies

Docking was performed on 135 ZAP-70 inhibitors and also on hits retrieved from virtual screening using GOLD. Fifty distinct poses of each ligand in the active site of ZAP-70 were generated. Gold Fitness scores were compared with observed activity for all molecules which were found to correlate well with the biological activities (135 molecules, $r = 0.712$). The correlation coefficient is r^2, which equals to 0.507 and this value is indicative of correlation. The most active molecules are found to have a very high fitness score. It was also observed that hydrogen bond interactions play a major role in deciding the fitness score of the molecule. A better understanding of the interactions is obtained by viewing the molecules in the active site. The most energetically favorable conformation for molecule **34** in the ZAP-70 complex is shown in Fig. 6. It forms different binding interactions with the amino acids in the hinge region and other active site amino acids of the ZAP-70 complex. The aromatic C–3H atom of phenyl ring formed hydrogen bond with backbone carbonyl group of MET416 with an interaction distance of

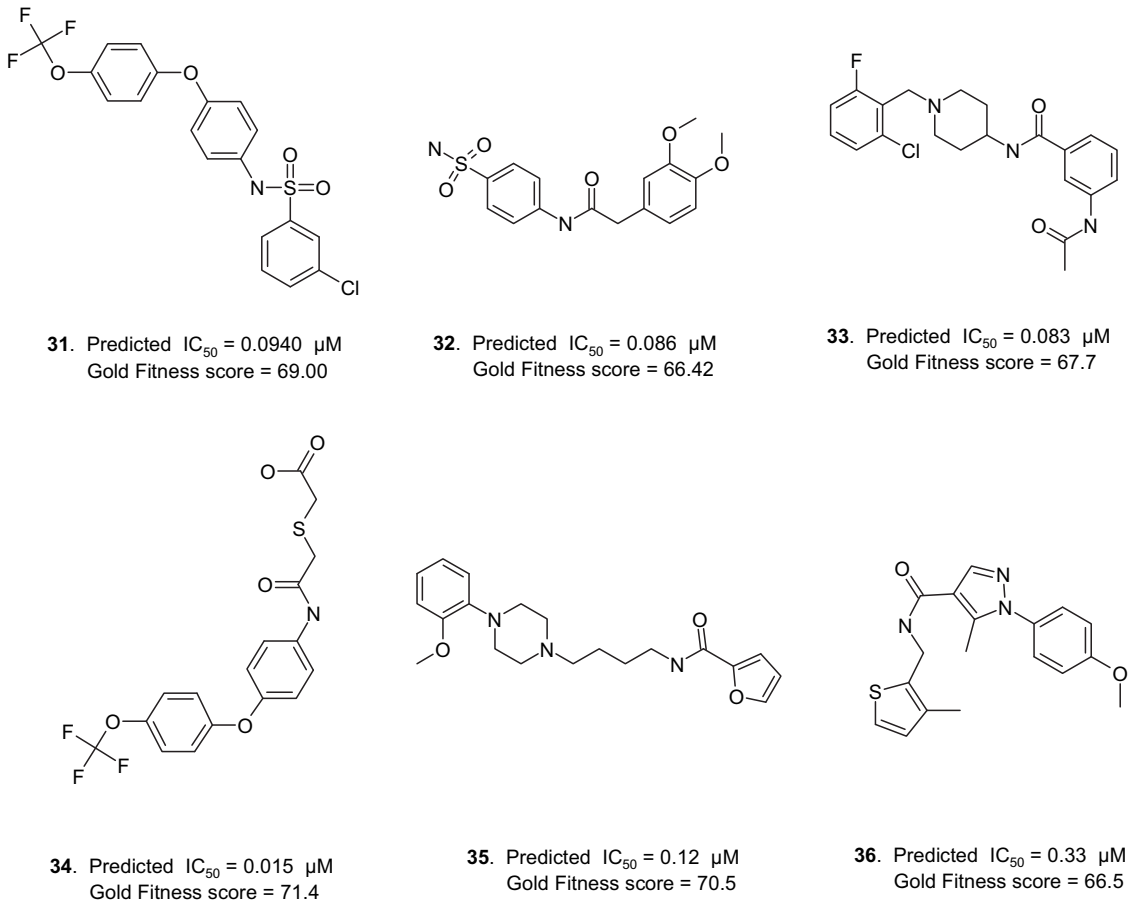

31. Predicted IC_{50} = 0.0940 μM
Gold Fitness score = 69.00

32. Predicted IC_{50} = 0.086 μM
Gold Fitness score = 66.42

33. Predicted IC_{50} = 0.083 μM
Gold Fitness score = 67.7

34. Predicted IC_{50} = 0.015 μM
Gold Fitness score = 71.4

35. Predicted IC_{50} = 0.12 μM
Gold Fitness score = 70.5

36. Predicted IC_{50} = 0.33 μM
Gold Fitness score = 66.5

Fig. 5. Lead molecules retrieved from the NCI database as potent ZAP-70 inhibitors along with its pharmacophore predicted IC_{50} and Gold Fitness score values.

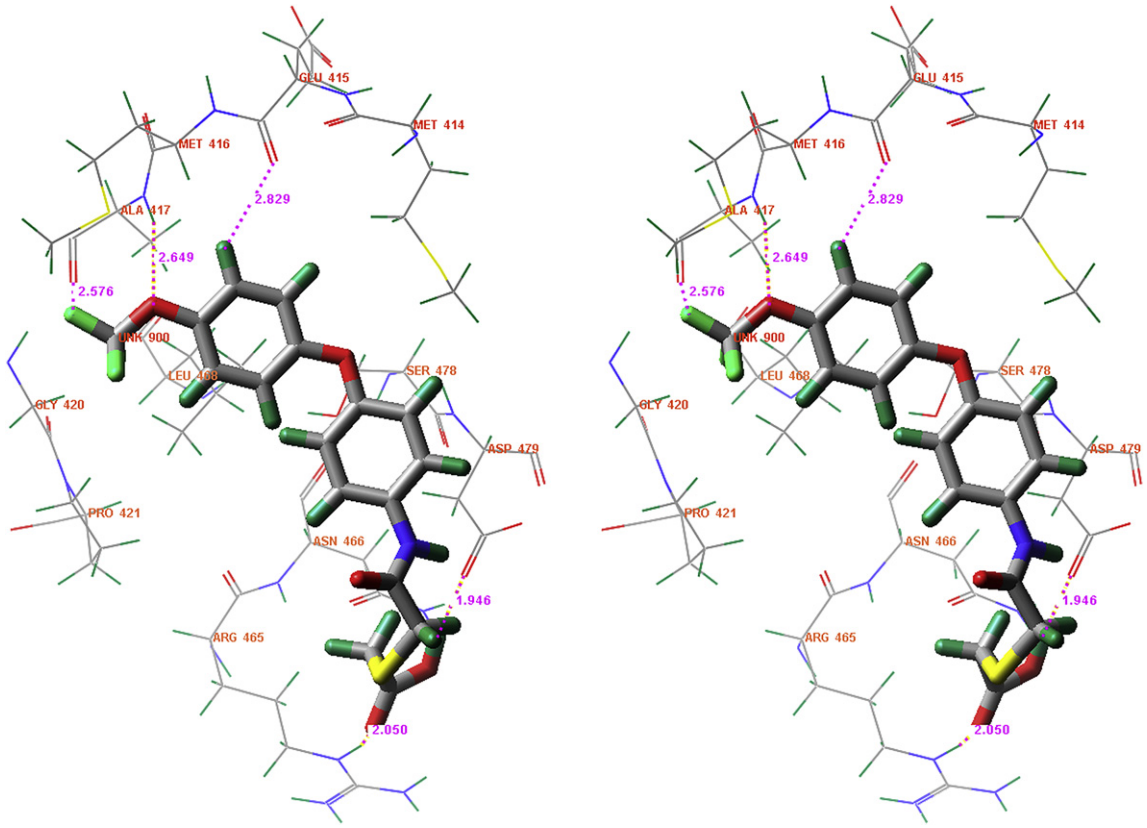

Fig. 6. Stereo view of the binding mode of molecule **34** in the ATP-binding site of ZAP-70, suggested by molecular docking studies. Molecule **34** and its H-bonding patterns (GLY418, MET416, ALA417, ARG465 and ASP479) are represented in stick model. The key H-bonds between **28** and ZAP-70 are indicated by the pink dotted lines, together with the bond lengths in angstroms. The atoms are colored as follows: H, green; O, red; N, blue; C, grey; F, light green.

2.829 Å. The oxygen of trifluoro methoxy group interacts with backbone amino group of ALA417 with an interaction distance of 2.649 Å. Similarly, fluorine atom of trifluoro group is interacting to backbone carbonyl group of GLY418 with distance of 2.576 Å. The aliphatic C–H atom of methylene group formed hydrogen bond with side chain carbonyl group of ASP479 with an interaction distance of 1.946 Å. The carbonyl of carboxylic acid formed H-bond with amino of side chain guanidine group of ARG465 with an interaction distance of 2.050 Å. Most of the inhibitors had bulky substituents interacting with the hydrophobic pocket. In addition, it was observed that docking could limit the number of false positive hits compared to Hypo1. Interestingly, the pharmacophore and docking models showed complementary behavior in limiting the number of false positive and false negative hits. The overlay of the docking pose of enzyme with its corresponding pharmacophore features is shown in Fig. 7.

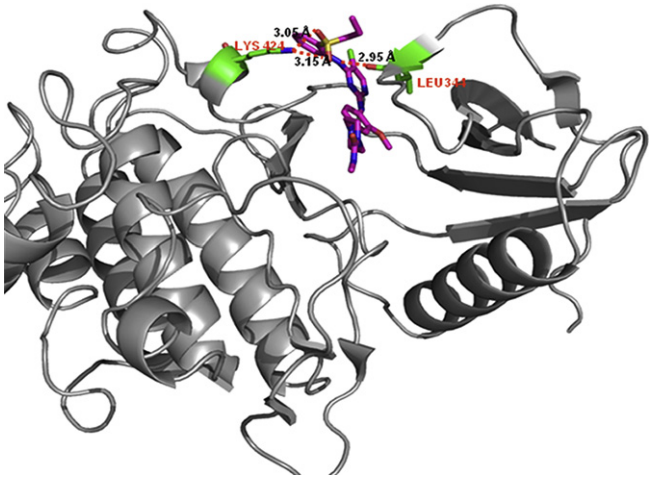

Fig. 7. Overlay of the docking pose of enzyme with pharmacophore features.

4. Conclusion

The pharmacophore models were capable of predicting the activities over a wide variety of scaffolds and thus can be used as (1) three-dimensional query in database searches to identify compounds with diverse structures that can function as potent inhibitors and (2) to evaluate how well any newly designed compound maps to the pharmacophore before undertaking any further study including synthesis. Both these applications may help in identifying or designing compounds for further biological evaluation and optimization. Pharmacophore studies indicate that the best inhibitor model consists of (1) one hydrogen bond acceptor, (2) one hydrogen bond donor (3) one hydrophobic aliphatic and (4) one hydrophobic aromatic features. The most active molecule in the training set fits very well with the top scoring pharmacophore hypothesis. Virtual screening produced some false positives and a few false negatives. It is believed that concurrent use or a consensus study, which readily minimizes these errors, could be an added tool for pharmacophore model based virtual screening in order to produce reliable true positives and negatives. GOLD docking studies show the important interactions which the potent

inhibitors have with the active site residues. The pharmacophore model is further used to screen putative molecules from the NCI database. An astute blend of pharmacophore analysis, docking procedures and database search has resulted in predicting putative novel inhibitors of the ZAP-70 complex.

References

[1] E. Arpaia, M. Shahar, H. Dadi, A. Cohen, C.M. Roifman, Cell 76 (1994) 947–958.
[2] E.W. Gelfand, K. Weinberg, B.D. Mazer, T.A. Kadlecek, A. Weiss, J. Exp. Med. 182 (1995) 1057–1065.
[3] R.L. Wange, N. Isakov, T.R. Burke, A. Otaka, P.P. Roller, J.D. Watts, R. Aebersold, L.E. Samelson, J. Biol. Chem. 270 (1995) 944–948.
[4] A.C. Chan, T.A. Kadlecek, M.E. Elder, A.H. Filipovich, W.L. Kuo, M. Iwashima, T.G. Parslow, A. Weiss, Science 264 (1994) 1599–1601.
[5] M.E. Elder, D. Lin, J. Clever, A.C. Chan, T.J. Hope, A. Weiss, A.T.G. Parslow, Science 264 (1994) 1596–1599.
[6] K. Nishikawa, S. Sawasdikosol, D.A. Fruman, J. Lai, Z. Songyang, S.J. Burakoff, M.B. Yaffe, L.C. Cantley, Mol. Cells 6 (2000) 969–974.
[7] L.A. Fernandez, J. Torrealba, G. Yagci, N. Ishido, M. Tsuchida, H. Tae Kim, Y. Dong, T. Oberley, J. Fechner, M.J. Colburn, J. Schultz, T. Kanmaz, H. Hu, S.J. Knechtle, M.M. Hamawy, Transplantation 74 (2002) 1609–1617.
[8] L. Jin, S. Pluskey, E.C. Petrella, S.M. Cantin, J.C. Gorga, M.J. Rynkiewicz, P. Pandey, J.E. Strickler, R.E. Babine, D.T. Weaver, K.J. Seidl, J. Biol. Chem. 279 (2004) 42818–42825.
[9] H. Hisamichi, R. Naito, A. Toyoshima, N. Kawano, A. Ichikawa, A. Orita, M. Orita, N. Hamada, M. Takeuchi, M. Ohta, S. Tsukamoto, Bioorg. Med. Chem. 13 (2005) 4936–4951.
[10] G.W. Krystal, S. Honsawek, D. Kiewlich, C. Liang, S. Vasile, L. Sun, G. McMahon, K.E. Lipson, Cancer Res. 61 (2001) 3660–3668.
[11] M. Eric, Z. Lilu, US 20050171076 A1, 2005.
[12] C. Garcia-Echeverria, T. Kanazawa, E. Kawahara, K. Masuya, N. Matsuura, T. Miyake, O. Ohmori, I. Umemura, R. Steensma, G. Chopiuk, J. Jiang, Y. Wan, Q. Ding, Q. Zhang, N.S. Gray, D.S. Karanewsky, WO 2005/016894 A1, 2005.
[13] D. Peter, David D.F.C. Moffat, M.J.M. Davis, M.C. Hutchings, US 5958935 A, 1999.
[14] Catalyst User Guide, Accelry's Software Inc., San Diego, 2005.
[15] O.O. Clement, A.T. Mehl, in: F.O. Guner (Ed.), Pharmacophore Perception, Development, and Use in Drug Design – IUL Biotechnology Series, International University Line, La Jolla, California, 2000, pp. 71–84.
[16] P.W. Sprague, R. Hoffmann, in: H. Van de Waterbeemd, B. Testa, G. Folkers (Eds.), Computer Assisted Lead Finding and Optimization – Current Tools for Medicinal Chemistry, VHCA, Basel, 1997, pp. 230–240.
[17] D. Barnum, J. Greene, A. Smellie, P. Sprague, J. Chem. Inf. Comput. Sci. 36 (1996) 563–571.
[18] H.M. Berman, J. Westbrook, Z. Feng, G. Gilliland, T.N. Bhat, H. Weissig, I.N. Shindyalov, P.E. Bourne, Nucleic Acids Res. 28 (2000) 235–242.
[19] Cerius^2, Version 4.11, Accelrys Inc., San Diego, California, USA, 2005.
[20] G. Jones, P. Willett, R.C. Glen, J. Mol. Biol. 245 (1995) 43–53.
[21] A. Hirashima, M. Morimoto, E. Kuwano, E. Taniguchi, M. Eto, Bioorg. Med. Chem. 10 (2002) 117–123.
[22] O.F. Guner, D.R. Henry, in: Osman F. Guner (Ed.), Pharmacophore Perception, Development, and Use in Drug Design, International University Line, La Jolla, California, 2000, pp. 193–210.